

## Assessment of Human Red Blood Cell Aggregation Using Image Processing and Wavelets

A. Kavitha, S. Ramakrishnan

Department of Instrumentation Engineering, MIT Campus, Anna University,  
Chennai - 600 044, India. Email: ramki@mitindia.edu

**Abstract.** Aggregation of red blood cells which manifests in the form of rouleaux is a major determinant of flow behavior of blood in both micro and macro circulation. Any alteration in the normal behavior is found to be a critical factor in plugging of arterioles and venules forming irreversible clumps. In this work, the aggregation behavior of red blood cells is analyzed using Wavelet transforms. The artificially induced red cell aggregate images obtained from normal adult volunteers are used for the study. An arbitrary aggregation size index is derived using four different wavelet functions. The results demonstrate the ability of wavelets to precisely differentiate variations in degree of aggregation and their intercellular bonding. Also the aggregation size indices are found to be similar and consistent for a given aggregate for all wavelet functions. As the association and dissociation of red cells and the bonding strength during cluster formation are direct indicators of altered flow behavior of red cells in micro-vessels and large arteries such analysis seems to be clinically relevant. The methodology, algorithm and observations based on Wavelet transforms are discussed in detail.

**Keywords:** Red cell aggregates, Wavelet Transform, inter- erythrocytic cohesive forces, aggregation index

### 1. Introduction

The most significant factors responsible for micro and macro circulatory blood flow disorders are enhanced red blood cell aggregation, increased plasma viscosity and lowered erythrocyte deformability [16, 25]. Under physiological conditions the red blood cells in static or slowly moving blood, adhere face to face like piles of coins to form reversible cell-to-cell contact leading to formation of aggregates. The measurement of red blood cell aggregation could be used to quantify physiologically significant rheological properties. Red cell aggregation increases blood viscosity and thus affects the passage of the cells through micro vessels, especially in venules with low shear flow [28]. In conditions arising due to pathological states aggregates are capable of plugging arterioles and venules [6]. Abnormal red cell aggregation has been found to be associated with several diseases and conditions, which include diabetics, malaria, cardiovascular malfunction, lacunar brain infarcts, essential hypertension, and immunoglobulin and hematological disorders, local anesthesia and many others [18, 19]. Therapeutic interventions, which affect RBC aggregation, are now becoming available and these include rheopheresis, aspirin and statins [4]. Thus aggregation of red cells is a major determinant of flow properties of blood in microcirculation and of practical significance in health care [27].

The various methods of analyzing aggregation include Erythrocyte sedimentation rate test, Ultrasonic back-scattering technique, Microscopic counting techniques and Optical methods [23]. Over the recent years a number of optical methodologies have been proposed to quantify the formation of red blood cell aggregates. The Myrenne erythrocyte aggregometer is the simplest but is limited in sensitivity [21]. Hitt and Lowe [12] used Fourier methods to

examine the spatial patterns of transmitted light intensities of in vitro aggregating blood flow and of computer simulated aggregating flows. But the analysis was capable only of providing approximate bounds for the aggregate sizes due to the broadness of the Fourier spectrum. Image processing has been employed in the automated diagnosis and classification of malaria on thin blood smears [26].

Wavelet transforms are multiresolution representations of images. They decompose images into multiscale details according to an orthonormal basis function called wavelet function [15, 30] and in decomposing an image into frequency bands; the width of the band is determined by a dyadic scheme. The image is decomposed in frequency channels of constant bandwidth on a logarithmic scale at any required level. This particular way of dividing frequency bands matches the statistical properties of most images very well. Wavelets are capable of reporting structural information at different locations within the image. There has been active research in applying wavelets to various aspects of imaging informatics, including compression, enhancements, analysis, classification, retrieval and also in analyzing radiographic images in the detection of trabecular patterns in osteoporosis [29, 30] in recent years. Wavelets prove to be a useful tool in noise removal of medical images.

The discrete wavelet transform has advantages such as similarity of data structure with respect to the resolution and available decomposition at any level. There have been very few attempts in analyzing red cell aggregates using 1-D Continuous Wavelet transforms in simulated aggregates [17]. In this work, Two- Dimensional discrete wavelet Transforms are employed to study the aggregation behavior of the erythrocytes using digital images. Red cell aggregates with various degree of aggregation are analyzed using Wavelets and Aggregation Size Index (ASI), which defines the size of aggregates, is derived for various wavelet functions.

## 2. Images and Methodology

Blood samples for the study are obtained from healthy, adult volunteers ( $N=10$ ) at Klinikum der RWTH, Aachen, Germany as described elsewhere [18, 20]. The images are then processed using various image processing routines. They are rescaled to cover the entire dynamic range and are segmented to detect transitions, which differ greatly in contrast from the background image. Changes in contrast are detected by calculating the gradient of the image using sobel operator. The binary gradient mask image obtained after edge detection is dilated using the vertical structuring element followed by the horizontal structuring element. This segmentation algorithm finally clears the objects connected to the border of the image and smoothen the image with a diamond-structuring element.

The processed images are then subjected to Wavelet Transforms. Two-dimensional Discrete Wavelet Transforms is adopted (2-D DWT) in this work due to its fast computational algorithm for decomposition and the discrete nature of the image pixels [2]. Chosen wavelets from the Daubechies, Symlet, Cioflet and Biorthogonal families are employed. These wavelets have orthogonality or biorthogonality characteristics that allow for space saving code and fast execution [30]. Wavelet transforms refers to the decomposition of an image with a family of real orthonormal bases  $\Psi_m, n(x)$  obtained through translation and dilation of kernel function  $\Psi(x)$  known as the mother wavelet. For each integer  $r$ , the orthonormal basis for  $L_2(R)$  is defined as

$$\phi_{r,j,k}(x) = 2^{(j/2)\phi} \phi_r(2^j x - k), j, k \in \mathbb{Z} \quad (1)$$

Where the function  $\Phi_r(x)$  in  $L^2(R)$  has the property that  $\{\Phi_r(x-k)/k, k \in Z\}$  is an orthonormal sequence in  $L^2(R)$  [30]. Here,  $j$  is the scaling index,  $k$  is the shifting index and  $r$  is the filter index then the trend  $f_j$ , at scale  $2^{-j}$  of a function  $f \in L^2(R)$  is defined as

$$f_j(x) = \sum_k (f, \phi_{r,j,k}) \phi_{r,j,k}(x) \quad (2)$$

The details of  $r$  fluctuations are defined by

$$d_j(x) = f_{j+1}(x) - f_j(x) \quad (3)$$

Daubechies' orthonormal basis has the following properties,  $\Psi_r$  has the compact support interval  $(0, 2r + 1)$ ,  $\Psi_r$  has about  $r/5$  continuous derivatives

$$\int_{-\infty}^{\infty} \psi_r(x) dx = \int_{-\infty}^{\infty} x^r \psi_r(x) dx = 0 \quad (4)$$

where  $\Phi_r(x)$  - Father Wavelet and  $\Psi_r(x)$  - Mother Wavelet

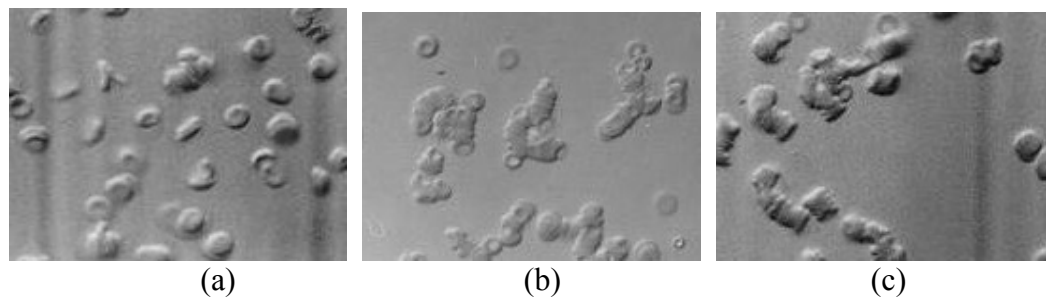


**Fig.1.** Typical red blood cell aggregates with increasing degree of aggregation. (a) mild aggregation (b) moderate aggregation (c)severe aggregation.

Figure 1 shows 3 representative aggregate images in their increasing order of aggregation with 1(a), 1(b) and 1(c) as samples of mild, medium and severe aggregations. Wavelet function decomposes the input aggregate image and their statistical evaluation result in generation of valuable parameters such as mean, median, mode and standard deviation. The aggregate samples of uniform image size and different degree of aggregation are decomposed at level 1 and 2 using various chosen wavelet functions such as Daubechies (Db), Symlet (Sym), Coiflet (Coif) and Bior and the corresponding horizontal detail coefficients with fixed form threshold are utilized to identify the aggregation size index. By several trials the standard deviation of the coefficients generated by the wavelet functions for a given image appeared to show significant variation. It was found to be linearly proportional to the size of the aggregate. Hence, this parameter was chosen to be the arbitrary index for aggregation size. Thus, Aggregation Size index (ASI) is the standard deviation of cumulative histograms of the pixel intensities of the horizontal detail coefficients decomposed at level 1 and 2 and analyzed using the various chosen wavelet functions.

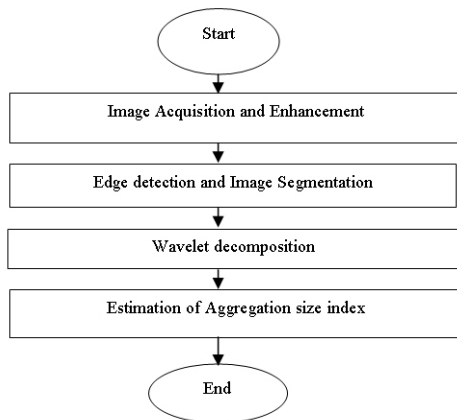


**Fig. 2** Sequence of processes involved in analyzing the aggregates of different bonding strengths.

The ratio of low frequency to high frequency components is determined and is identified as the index called Ratio Metric. Figure 2 shows the sequence of processes carried out in the derivation of the aggregation size index.

### 3. Results

Table 1 shows the derived aggregation size index values of ten aggregate samples with different size and degree of aggregation. Different wavelet functions are employed and the corresponding values obtained by decomposing the images at level 1 are tabulated. With the image size being constant for all the samples, the index is found to vary widely with aggregate size. A direct correlation of the index is met with the aggregate size. For samples with larger spans, the index values are also high. And the index value is found to decrease with aggregates of smaller spans. Though there is no consistency in the values of the coefficients obtained using different wavelets for the same sample, the discrimination in size is maintained for all wavelets. The mean value and standard deviation of the aggregation size indices derived through four different wavelet functions for typical four samples are presented in table 2. It is observed that the for all wavelet functions, similar aggregate size indices were observed.

Table 3 is the ratio of low frequency to high frequency components obtained for the wavelet functions decomposed at levels 1 and 2. This ratio metric value is also found to have a corresponding correlation with image sizes. But this correlation is found to define only the size of the aggregates and not on the intercellular spacing or degree of bonding of the aggregates.

Figures 3 and 4 show the variation of the derived aggregation size indices obtained for 4 aggregate samples of different sizes using Db5, Sym5, Coif5, Bior5.5 wavelets decomposed at levels 1 and 2. It is observed that all the chosen wavelet functions show consistent variations in the index values for an aggregate. The variation in ASI value among the various wavelet functions employed is consistent for both the decomposition levels for a given aggregate size.

**Tab. 1** Standard deviation of the cumulative histograms of the horizontal detail coefficients of 10 samples decomposed at level 1

Samples	Wavelet functions			
	Db 5	Sym 5	Coif 5	Bior 5.5
1	78.21	98.64	70.01	81.01
2	82.82	93.53	75.75	90.26
3	80.47	103.4	76.52	81.34
4	91.57	96.89	97.31	94.1
5	80.89	109.1	80.13	87.44
6	85.86	88.12	83.71	92.28
7	81.57	109.7	71.86	87.19
8	92.71	118.2	80.72	101
9	76.86	88.78	68.23	83.12
10	75.73	104.5	69.85	79.8

**Tab. 2** Mean and standard deviation of the aggregation size indices for 4 wavelet functions

Decomposition Levels	Mean $\pm$ SD of ASI for 4 wavelet functions			
	Sample 1	Sample 2	Sample 3	Sample 4
Level 1	81.66 $\pm$ 11.81267	85.59 $\pm$ 7.944621	98.16 $\pm$ 15.74537	79.247 $\pm$ 8.8119
Level2	98.39 $\pm$ 8.859274	113.09 $\pm$ 13.50498	123.3 $\pm$ 14.5421	103.283 $\pm$ 11.6637

**Tab. 3** Ratio metric of low frequency to high frequency components obtained for the wavelet functions decomposed at levels 1 and 2.

Samples	Level 1				Level 2			
	Db 5	Sym 5	Coif 5	Bior 5.5	Db 5	Sym 5	Coif 5	Bior 5.5
1	10.31	4.269	3.88	3.819	1.39	0.9279	1.139	0.951
2	10.03	4.092	3.808	3.455	1.58	0.808	1.313	0.969
3	11.47	4.52	4.52	4.232	1.597	1.286	1.71	1.24
4	10.32	4.49	4.22	3.88	1.405	0.703	1.31	0.874
5	10.87	4.65	5.187	3.96	1.42	0.740	1.64	0.856
6	10.52	4.663	4.7	4.12	1.66	1.033	1.61	1.12
7	10.22	4.29	4.146	3.86	1.59	1.038	1.324	1.62
8	10.72	4.73	3.91	4.28	1.59	0.95	1.28	0.992
9	11.02	4.56	3.83	3.95	1.55	0.834	1.35	0.98
10	12.38	5.13	4.34	4.68	1.62	1.083	1.24	1.2

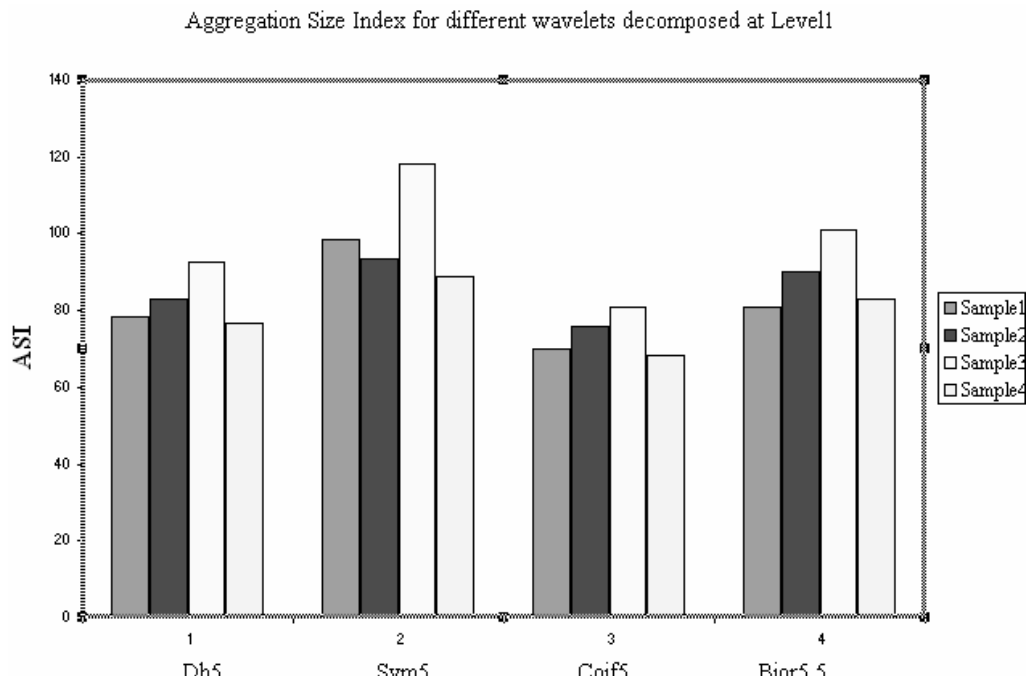


**Fig.3.** Variation of aggregation Size indices obtained for 4 samples of different sizes using various Wavelets decomposed at level 1.

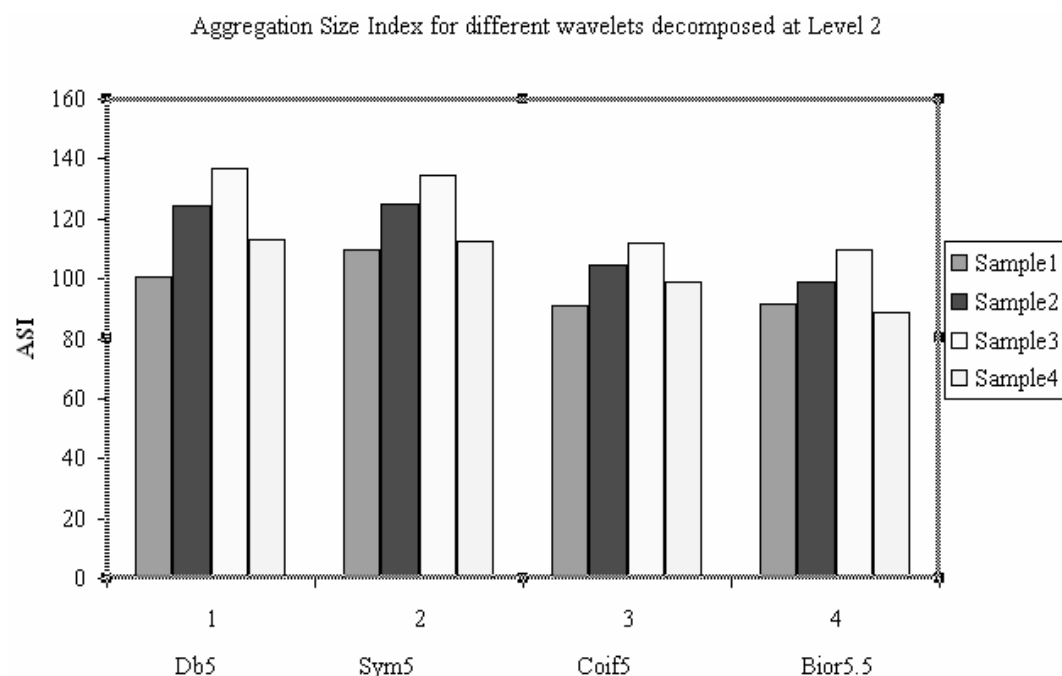


**Fig.4.** Variation of aggregation Size indices obtained for 4 samples of different sizes using various Wavelets decomposed at level 2.

#### 4. Conclusion

The phenomenon of red cell aggregation manifests itself mostly in the form of rouleaux and endows yield stress thereby affecting the microcirculatory flow. The rate and degree of erythrocyte aggregation depends on the suspending medium, physico-chemical properties and flow conditions [1]. The adhesive force between red cells in blood flow tends to draw them towards the center of the flow excluding the other cell types towards walls and increases

interaction with the vessel endothelium [10]. The interaction between forward blood flow, downward sedimentation of aggregates and local hemoconcentration due to transcapillary filtration greatly influences the kinetics of aggregate formation in vivo and its consequences [27]. All these effects present in the normal individual are exaggerated with the enhancement in aggregation due to a wide variety of pathologies. Intensity of aggregation has been used as an index of the severity of such as cardiovascular diseases, diabetes mellitus, occlusive diseases and microangiopathy [24]. Also superimposed red blood cells might appear as aggregates, which lead to misinterpretation of aggregate concentrations. Thus the actual erythrocyte aggregability is a significant prognostic sign in determining the disease stages [16].

Aggregation indices have been analyzed using various techniques but there are only few reports on methods to distinguish aggregates based on their size and intercellular spacing. In this work, the red blood cell aggregate images of various sizes artificially induced in normal adult samples are analyzed. An attempt has been made to identify the intercellular spacing and intensity using various wavelet functions. There are earlier reports on analysis of simulated aggregates employing 1-D wavelet [17]. In the present work red cell aggregates with varied sizes are analyzed using 2-D Discrete Wavelet Transforms by decomposing them at two levels. The effectiveness of wavelet functions is assessed through aggregation size index and it is found that the indices are similar and consistent for a chosen size of the aggregates. The analysis of low and high frequency components obtained using wavelet decompositions along with the calculated ratio metric values seems to yield useful information on the size of the aggregates.

Since aggregation of red cells is a major determinant of flow properties of blood in microcirculation, studies on automated methods to assess size and index of aggregation are essential for clinical evaluation [27]. Only very few attempts are made on assessing the intercellular spacing in aggregates which is a significant factor contributing to the adhesion strength. Wavelets have proven to be effective in investigating cell shapes and even the sharp transitions in images were preserved and depicted extremely well in wavelet expansions [13]. From the results it appears that our method of analyzing red blood cell aggregates by 2-D wavelet transforms taking into account the intensity of aggregation might be of better clinical significance. Since the size of aggregation and the inter- erythrocytic cohesive forces are analyzed by considering aggregates of different sizes and different bonding strengths, severity of pathological conditions could also be assessed. The derived aggregation size index obtained for various aggregate strengths could be an indication of cell population and this could assist therapeutic measures. Such observations made continuously with respect to time would provide insight into dynamics of aggregates and would enable to automate the process and observe online.

## Acknowledgement

One of the authors (SR) acknowledges DAAD, Bonn, Germany (DAAD Award 422/ind-4-tzn/95), Institute of Physiology, RWTH, Aachen and Dr. Sances Research Foundation in Biomedical Engineering, USA for their support.

## References

- [1] Aggelopoulos E. G., Karabetsos E. and Koutsouris D., In Vitro Estimation of Red Blood Cells Aggregation using Ultrasound Doppler Techniques, Clin. Hemorheol. Microcirc., 17, 107- 115, 1997.

- [2] Aldroubi A. and Unser M. A., Wavelets in medicine and Biology, , Boca Raton, FL: CRC, 1996.
- [3] Artmann G., A microscopic photometric method for measuring erythrocyte deformability, *Clin. Hemorheol.*, 6, 617- 627,1986.
- [4] Berliner S., Ben- Ami R., Samocha-Bonet D., Abu- Abeid S., Schechner V., Beigel Y., Shapira I., Yedgaur S. and Barshtein G., The degree of red blood cell aggregation on peripheral blood glass slides corresponds to inter- erythrocyte cohesive forces in laminar flow, *Thrombosis res.*, 114, 37-44,2004.
- [5] Boynard M. and Goldstein J. M., Ultrasound Blood Characterization. Acoustical Imaging, *Clin. Hemorheol. Microcirc.*,10, 315- 324, 1982.
- [6] Chien S. and Jan K. M., Ultrastructural Basis of the Mechanism of Rouleaux Formation, *Microvasc. Res.*, 5, 155-166, 1973.
- [7] Chien S., Biophysical Behavior of red blood cells in suspensions, in: *The Red Blood Cell*, D. Surgenor,(Ed.), Academic Press, New York, 1031- 133, 1975.
- [8] Chien S., Sung L., Burke A. and Usami S., Determination of Aggregation Force in Rouleaux by Fluid Mechanical Technique, *Microvasc. Res.*, 13, 327- 333, 1977.
- [9] Chien S., King R., Schuessler G., Skalak R., Tozeren A., Usami S., and Copley A., *Biorheology*, *Aiche Symposium Series*, 74, 56- 60, 1978.
- [10] Chien S. and Sung L. A., Physicochemical basis and clinical and clinical implications of red cell aggregation, *Clin.Hemorheol.*,7, 71,1987.
- [11] Deuticke B., Transformation and restoration of biconcave shape of human erythrocytes induced by amphiphilic agents and changes of ionic environment, *Biochim. Biophys. Acta.*, 163, 1968, 494- 500.
- [12] Hitt D. L. and Lowe M. L., Spatial Analysis of Red Blood Cell Aggregation for in vitro tube flow, *Proc. World Cong. on Microcirc.*, Messmer, K and Kubler, W. M., (Eds.), Monduzzi Editore, Bologna, Italy, 207- 211, 1996.
- [13] Kavitha A. and Ramakrishnan S., Analysis on the erythrocyte shape changes using wavelet transforms, *Clin. Hemorheol. Microcirc.*, 33, 327- 335, 2005.
- [14] Khare A. and Tiwary U. S., Soft- thresholding for denoising of medical images- A multiresolution approach, *Intl. Journ. Wavelets, Multires. Inform. Process.* 3, 477-496, 2005.
- [15] Kumar D. K., Pah N. D. and A. Bradley, Wavelet analysis of Surface Electromyography to determine Muscle Fatigue, *IEEE Trans. on Neural Sys. and Rehab. Eng.*, 11, 400-406, 2003.
- [16] Mchedlishvili G., Varazashvili M., Mamaladze A. and Momtselidze N., Bloodflow structuring and its alterations in the capillaries of the cerebral cortex, *Micro Vasc. Res.*, 53, 201-210,1997.
- [17] Prabhu R. D., Darren L. H. and Charles D. E., Wavelet Analysis of Red Blood cell Aggregate Structures, *Proc. Bioengg. Conf.*, ASME, BED American Society of Mechanical Engineers, 50, 473- 474, 2001.
- [18] Ramakrishnan S., Grebe R., Megha Singh, and Schmid- Schönbein H., Aggregation of shape altered erythrocytes: An in vitro study, *Current Sci.*, 77, 805-808, 1999.
- [19] Ramakrishnan S., Grebe R., Megha Singh, and Schmid- Schönbein H., Analysis of risk factor profile in plasmacytoma patients, *Clin. Hemorheol. Microcirc.*, 20, 20- 25, 1999.
- [20] Ramakrishnan S., Degenhardt R., Vietzke K., Grebe R., Megha Singh and Schmid- Schönbein H., Influence of immunoglobulin G and immunoglobulin A on erythrocyte aggregation: a comparative study, *ITBM- RBM*, 22, 241-246, 2001.
- [21] Rampling M. W. and Whittingstall P., A Comparison of five methods for estimating red cell aggregation, *Klin. Wochensch.*, 64, 1084- 1088, 1986.

- [22] Rampling M. W., Quantization of Rouleaux Formation- A Useful Clinical Index, Rev. Port. Hemorheol., 1, 41- 49, 1987.
- [23] Rampling M. W., Plasma- Protein Induced Aggregation of Erythrocytes: Its causes, Estimation and Effects of Blood Flow, Studia Biophys.,134, 91-94,1989.
- [24] Rampling M. W., Red Cell Aggregation as a Risk factor for Thrombosis, Rev. Port. Hemorheol., 5, 39- 47,1991.
- [25] Rampling M. W., Meiselmann H. J., Neu B. and Baskurt O. K., Influence of cell-specific factors on red blood cell aggregation , Biorheology, 41, 91- 112, 2004.
- [26] Ross N. E., Pritchard C. J., Rubin D. M. and Dusé A. G., Automated image processing method for the diagnosis and classification of malaria on thin blood smears, Med. Biol. Eng. Comput., 44, 427- 436,2006.
- [27] Schmid- Schönbein H., Malotta H. and Striesow E., Erythrocyte Aggregation: Causes, Consequences and methods of assessment, Tijdschr NVKC, 15, 88- 97, 1990.
- [28] Suzuki Y., Tateishi N., Cicha I. and Maeda N., Aggregation and Sedimentation of mixtures of Erythrocytes with different properties, Clin. Hemorheol. Microcirc., 25 105- 117, 2001.
- [29] Faber T. D., Yoon D. C., Service S. K. and S. C. White, Fourier and Wavelet analysis of dental radiographs detect trabecular changes in osteoporosis, Bone, 35, 403- 411, 2004.
- [30] Wang J. Z., Wavelets and Imaging Informatics: A Review of the Literature, J. Biomed. Informat., 34, 129-141, 2001.